SCIENTIFIC AND TECHNICAL SECTION

Effect of Grinding Conditions of a TC4 Titanium Alloy on Its Residual Surface Stresses

J. Li, Y. Jia, N. Shen,[1] **Z. Yu, and W. Zhang**

Shanghai Key Laboratory of Mechanical Automation and Robotics, School of Mechatronics Engineering and Automation, Shanghai University, Shanghai, China

[1] shny@shu.edu.cn

The grindability of titanium alloys that are classified as hard-to-machine materials is studied in high-speed cylindrical grinding using a cubic boron nitride (CBN) wheel. The investigation is concerned with residual surface stresses, including the construction of its empirical model, orthogonal experiments with a CBN grinding wheel at a speed of 45–150 m/s, and prediction with the back propagation (BP) network. The results of residual surface stress measurements obtained in grinding experiments and of simulation analysis for five sets of grinding conditions are compared, it can be seen that the empirical model is partially applicable to a Ti-6Al-4V titanium alloy (TC4) under examined grinding conditions. Generally, the calculation results with the empirical model exhibit a significant deviation from the data of actual measurements in some cases. The BP network possesses the function of complex nonlinear mapping and adaptive learning. So the BP network is adopted to predict the relation between residual surface stresses and three key grinding conditions accurately enough. The accuracy of the network is verified, which lays the foundation for its in practical application.

Keywords: titanium alloy, high speed cylindrical grinding, surface residual stress, BP neural network, empirical model.

Introduction. Titanium alloys are difficult to grind due to their poor thermal properties and high chemical activity. The primary challenges in grinding titanium alloys are: the high specific energy, the high temperature in grinding area as well as the heavy grinding wheel adhesion and wear. Grinding is a common finishing method for titanium material, in order to obtain a precise surface quality. The surface residual stress is one of the main evaluations indices of the surface quality, which has a high impact on the performance [1, 2] of the workpiece. Lin and Lee [3] studied the effect of tool flank wear on the surface residual stresses of the machined surface. Ee et al. [4] used the finite element method to investigate the impact of sequential cuts, cutting conditions, etc., on the residual stresses induced by orthogonal machining. Vosough et al. [5] investigated the impact of high-pressure water-jet on the surface residual stress and concluded that the high-pressure jet increases the level of residual compression stresses in both cutting and feed directions, and thus the high-pressure water jet-assisted machining of titanium alloys is beneficial. Kang and Ren [6] analyzed the causes of the grinding residual stress of Ti-alloy specimen and optimized the grinding residual stresses of titanium alloy by selecting the reasonable grinding conditions, CBN grinding wheel and using the high-quality grinding fluid with extreme-pressure (EP) agent. Hu and Yuan [7] analyzed the forming mechanism of residual

stresses produced in the grinding process and concluded that higher constraints to the deformation in grinding process generate lower residual stresses, while the wheel material can diffuse into the surface layer of the workpiece to increase the compressive residual stresses.

The cylindrical grinding process (with grinding wheel speed v_s from 45 to 150 m/s) of titanium alloy TC4 is studied in this paper to find the suitable grinding conditions by orthogonal experiment, including grinding wheel speed v_s, workpiece speed v_w, and cutting depth a_p, for generation of higher surface residual compressive stresses. Then variance analysis of the experimental data is conducted to get the significant degree of influence of all the grinding conditions on the surface residual stresses. The experimental data are incorporated into the general model to identify the model parameters, so that the empirical model is determined in each particular case. The respective empirical model is adopted to examine the relationship between the surface residual stress and the grinding conditions. However, the empirical model cannot accurately describe the actual situation. A BP neural network is used to predict the surface residual stresses, which are compared with the calculated values of the empirical model and the experimental data, respectively. The results obtained using the networks are also compared and analyzed by using two different normalization methods. The network reliability and accuracy are verified by the comparative analysis of the results and the simulation process is presented, which can provide further guidance for production and processing.

1. Empirical Model of the Surface Residual Stress. Since the model of surface residual stress cannot be established accurately, the empirical model as shown in Eq. (1) has been adopted to describe the relationship between grinding conditions and surface residual stress

$$\sigma_1 = C v_s^{b_1} a_p^{b_2} v_w^{b_3}, \tag{1}$$

where σ_1 is the surface residual stress, C is a constant depending on the machined materials and grinding conditions, v_s is the grinding wheel speed, a_p is the cutting depth, v_w is the workpiece speed, and b_1, b_2, and b_3 are the undetermined coefficients.

Identification of parameters should be conducted under certain grinding conditions to explain the change between the objective function and experiment conditions. For example, Ren and Wang [8] proposed the empirical model of the surface residual stress generation under the set conditions, when GC60KV grinding wheel is used for grinding of the titanium alloy. However, the CBN grinding wheel used in this experiment is a super hard grinding wheel without the size effect. During a short-time continuous grinding with a CBN grinding wheel, the initial grinding force and specific grinding energy drop after dressing from high values to steady ones, which also reduces the titanium alloy deformation due to grinding. The grinding heat and non-uniform plastic deformation are the main factors, which influence the residual stresses in the grinding process [9]. Thus, the application of CBN grinding wheel for grinding of titanium alloy can allow one to avoid the chips adhering to the grinding wheel and the high grinding temperature, which contributes to the optimization of the surface residual stresses of the workpiece.

Equation (1) can be converted into a linear function as follows:

$$y = b_0 + b_1 x_1 + b_2 x_2 + b_3 x_3, \tag{2}$$

where $y = \log|\sigma_1|$, $b_0 = \log C$, $x_1 = \log v_s$, $x_2 = \log a_p$, and $x_3 = \log v_w$; while the linear relationship between the independent variables x_1, x_2, x_3 and the dependent variable y can be expressed by the following matrix equation:

$$Y = X\beta + \varepsilon, \tag{3}$$

where ε is the test error, β is the coefficient of independent variables, X is the independent variable, and Y is the dependent variable. The grinding experiments are required to determine the conditions in Eq. (3), and the vector representation of the corresponding terms in Eq. (3) is as follows:

$$Y = \begin{bmatrix} y_1 \\ y_2 \\ y_3 \\ \vdots \\ y_n \end{bmatrix}, \qquad X = \begin{bmatrix} 1 & x_{11} & x_{12} & x_{13} \\ 1 & x_{21} & x_{22} & x_{23} \\ 1 & x_{31} & x_{32} & x_{33} \\ \vdots & \vdots & \vdots & \vdots \\ 1 & x_{n1} & x_{n2} & x_{n3} \end{bmatrix}, \qquad \beta = \begin{bmatrix} \beta_0 \\ \beta_1 \\ \beta_2 \\ \beta_3 \end{bmatrix}, \qquad \varepsilon = \begin{bmatrix} \varepsilon_1 \\ \varepsilon_2 \\ \varepsilon_3 \\ \vdots \\ \varepsilon_n \end{bmatrix}.$$

2. Grinding Experiments and the Identification of Empirical Model Conditions.

2.1. Design of Grinding Experiments. The experiment is aimed to analyze the relationship between the surface residual stresses and grinding conditions, and then to determine the parameters of the empirical model.

A TC4 bar (Fig. 1a) of $\varnothing 80 \times 200$ mm is used in the grinding experiment. The high-speed CNC cylindrical grinding machine of model MGKS1332/H, and the vitrified bonded CBN grinding wheel with the maximum speed of 150 m/s (model 14Al-540-22-5 76N supplied by Saint-Gobain Abrasives Ltd.) are adopted. The cutting fluid of type CY-QX-17B is used to cool and lubricate the grinded surfaces. Dressing conditions of the wheel remain unchanged throughout the experimental process. Figure. 1b shows the experimental setup for investigation of surface residual stresses of titanium alloys under high-speed grinding conditions.

a   b
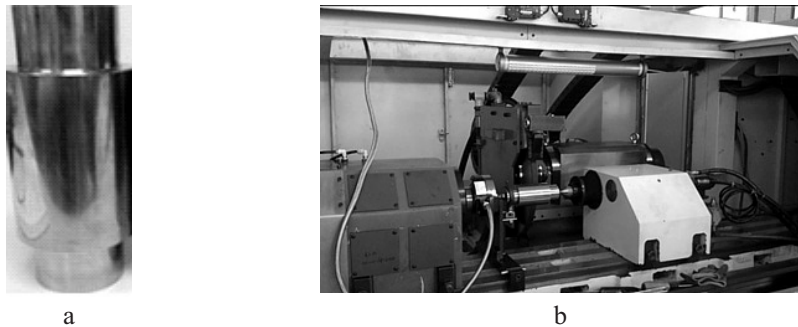
Fig. 1. The experimental workpiece and setup: (a) original workpiece (TC4); (b) high-speed CNC cylindrical grinding machine.

As is shown in Table 1, the orthogonal array is designed for grinding experiments to study the influence of three factors (grinding wheel speed v_s, workpiece speed v_w, and cutting depth a_p) with three (low, medium, and high) levels on the surface residual stresses. The experimental workpiece is subdivided into nine sections for the nine grinding experiments listed in Table 1. As shown in Fig. 2, the value of surface residual stresses in each processed section is measured by the X-ray diffraction (XRD) method [10, 11].

2.2. Analysis of Experimental Results. Under the different grinding process conditions, the curves shown in Fig. 3 describe the surface residual stresses in TC4 bar varying with the grinding wheel speed v_s, workpiece speed v_w, and cutting depth a_p, respectively.

In low-speed grinding (with grinding wheel speed between 45 and 60 m/s), the variation rates of the circumferential and axial surface residual stresses at grinding wheel speed v_s for TC4 are 9.750 and 0.250 MPa·s/m, respectively. Also in high-speed grinding (with grinding wheel speed between 60 and 94 m/s), the respective rates are 0.753 and

T a b l e 1

Experiment Number and Factor Level Details

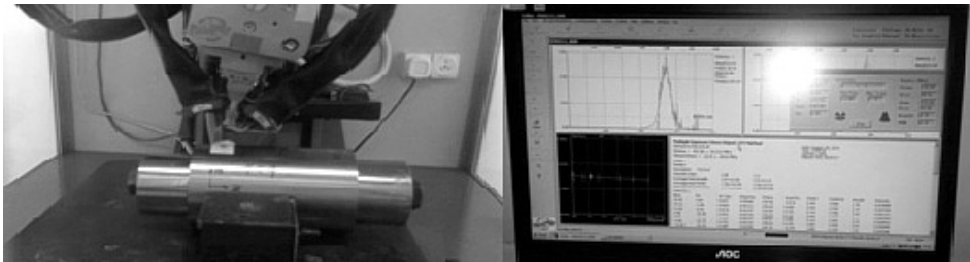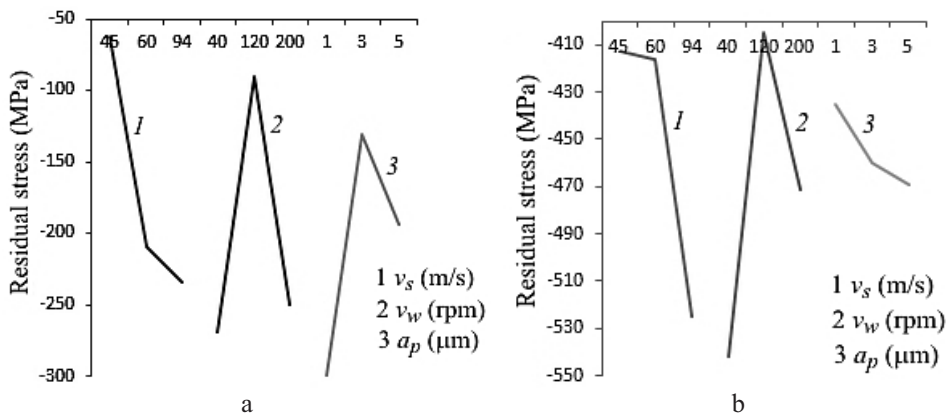| No. of grinding experiment	v_s, m/s	v_w, rpm	a_p, μm
1	45	40	1
2	45	200	5
3	45	120	3
4	60	120	5
5	60	40	3
6	60	200	1
7	94	40	5
8	94	120	1
9	94	200	3

Fig. 2. Surface residual stress measurement of TC4 workpiece.

Fig. 3. Variation of the circumferential (a) and axial (b) surface residual stresses of TC4 bar with the grinding wheel speed v_s, workpiece speed v_w, and cutting depth a_p.

3.191 MPa · s/m, respectively. In both cases, the surface residual stress is directly proportional to the grinding wheel speed v_s. As the workpiece speed v_w increases, the surface residual stresses increase after their drop, and the minimum value occurs at the workpiece speed v_w of 120 rpm. As the cutting depth a_p increases, the circumferential surface residual stress increases, in contrast to the axial one. As the cutting depth a_p increases, the surface residual stresses also increase after their drop, while the surface residual stress minimum value is attained at the cutting depth a_p of 3 μm.

Analysis of variance is conducted for the experimental conditions, which shows that the significant degrees of the grinding wheel speed v_s, cutting depth a_p, and workpiece

speed v_w, as the influence factors to the surface residual stress, are sorted in the decreasing order.

Grinding wheel speed v_s has the largest impact on the surface residual stresses. The significance level p of grinding wheel speed v_s is 0.4201 for the circumferential surface residual stress and 0.0099 for the axial one. This effect is attributed to the following factor: in high-speed grinding, the average undeformed chip thickness and the maximum undeformed thickness of a single CBN abrasive increase with the grinding wheel speed v_s, which results in the lower grinding force and grinding temperature. Thereby, the influence of the grinding thermal effect becomes more feeble than that of the burnishing effect, so that the residual stresses become higher. This result shows that the high-speed grinding can allow one to avoid grinding burns caused by the high temperature, and also to optimize the mechanical properties.

Cutting depth a_p has a feeble impact on the surface residual stress level. The significance level p of cutting depth a_p is 0.3241 for the circumferential surface residual stress and 0.0247 for the axial one. When the cutting depth a_p varies between 1 and 3 μm, the abrasives are so sharp that the grinding wheel is not easy to wear out. When the cutting depth a_p is higher than 5 μm, the plastic deformation and specific grinding energy increase. Moreover, this condition causes a phase transition and double quenching, when the workpiece is liquid-cooled, which reduces the surface residual stresses. In order to obtain the high compressive residual stress, the value of cutting depth a_p should be set as the mean value of its feasible range.

The workpiece speed v_w has the minimal impact on the surface residual stresses. The significance level p of workpiece speed v_w is 0.6129 for the circumferential surface residual stress and 0.0225 for the axial one. The influence of workpiece speed v_w on the residual stresses is in agreement for both directions. In particular, until the workpiece speed v_w reaches 120 rpm, the surface residual stress drops. When the workpiece speed v_w is higher than 120 rpm, the effect is the opposite. The main reason is as follows: when the workpiece speed v_w is low, the thickness of undeformed abrasive increases, which results in the grinding heat increase, so thermal effect has a larger impact than plastic deformation at this time; when the workpiece speed v_w further increases, the contact time between the grinding wheel and workpiece would decrease, and the grinding in this experiment accelerates the heat rate along the machined surface, which reduces the thermal effect.

2.3. Identification of the Empirical Model Parameters. In order to express the relationship between the surface residual stresses and grinding conditions qualitatively, the parameters of the empirical model are identified using the experimental results.

The data of the second, third, fifth, sixth, and eighth experiments that represent the characteristic of the total experimental scheme are selected for identification of the conditions, which are named as the first, second, third, fourth, and fifth conditional points.

Parameters β_0, β_1, β_2, and β_3 are estimated by the least-square method, and their estimated values are b_0, b_1, b_2, and b_3, respectively. The estimated values of the regression Eq. (2) can be written as follows:

$$\hat{y} = b_0 + b_1 x_1 + b_2 x_2 + b_3 x_3, \tag{4}$$

where $\hat{y}$ is the statistical variable, b_0, b_1, b_2, and b_3 are the regression coefficients obtained via the following equation:

$$b = (X'X)^{-1} XY. \tag{5}$$

The results on the residual stresses for 5 groups of measurements are incorporated into Eq. (2) and the results are as follows:

$$X = \begin{bmatrix} 1 & 1.653 & 0.477 & 2.079 \\ 1 & 1.778 & 0.699 & 2.079 \\ 1 & 1.778 & 0 & 2.301 \\ 1 & 1.973 & 0.699 & 1.602 \\ 1 & 1.973 & 0.477 & 2.301 \end{bmatrix}, \qquad Y = \begin{bmatrix} 2.615 \\ 2.599 \\ 2.639 \\ 2.734 \\ 2.705 \end{bmatrix}.$$

Then vectors X and Y are substituted into Eqs. (3) and (5) to yield the following results:

$$b = \begin{bmatrix} 2.185 \\ 0.364 \\ -0.062 \\ -0.079 \end{bmatrix}, \qquad |\varepsilon| = \begin{bmatrix} 20.910 \\ 24.264 \\ 11.558 \\ 0.974 \\ 15.739 \end{bmatrix}.$$

Therefore, the empirical model of the axial surface residual stress σ_z is expressed by Eq. (6):

$$\sigma_z = -153.073 v_s^{0.364} a_p^{-0.062} v_w^{-0.079}. \tag{6}$$

Similarly, the conditions of empirical model of the circumferential surface residual stress σ_z can be obtained and expressed by Eq. (7):

$$\sigma_z = -1.439 v_s^{1.714} a_p^{-0.794} v_w^{-0.343}. \tag{7}$$

In order to describe the relationship between the surface residual stress and grinding conditions more comprehensively, the data on the axial and circumferential surface residual stresses are combined for a joint comparative analysis by simulation based on the above empirical models.

3. Simulation of the Surface Residual Stresses. Trend analysis of the residual stresses can allow one to find the best combination of grinding conditions. The axial and circumferential residual stresses are analyzed, and the results of simulation study are shown in Figs. 4 and 5, respectively.

Figures 4 and 5 show that with the increase of the grinding wheel speed v_s, the circumferential residual stresses gradually exceed the axial ones. This phenomenon is more pronounced when the cutting depth a_p is small because the grinding direction is circumferential. A high temperature can be avoided due to the large contact area between the grinding wheel and workpiece, and the influence of thermal effect is weakened when the grinding wheel speed v_s is very strong. It is also known that the less the cutting depth a_p, the smaller the plastic deformation in the axial direction.

In order to improve the surface quality of the machined titanium alloy workpiece, the highest grinding wheel speed v_s, the lowest workpiece speed v_w, and the medium cutting depth a_p in its feasible range should be adopted in the grinding machine. This machining strategy is beneficial to producing the residual compressive stresses or at least limiting the maximum amplitude of the residual tensile stresses.

4. Prediction of Surface Residual Stress by BP Neural Network. The BP neural network is a kind of multilayer feedforward neural network, whose main features are signals forward transfer and the error back propagation [12]. Each neuron without feedback link only feeds forward to all neurons of the next layer. BP algorithm consists of two parts:
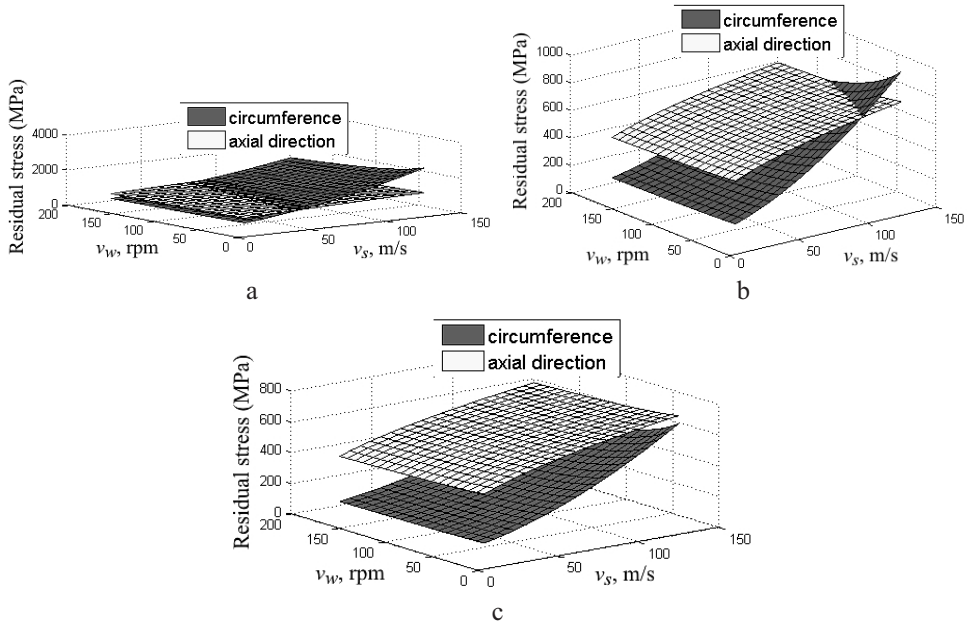
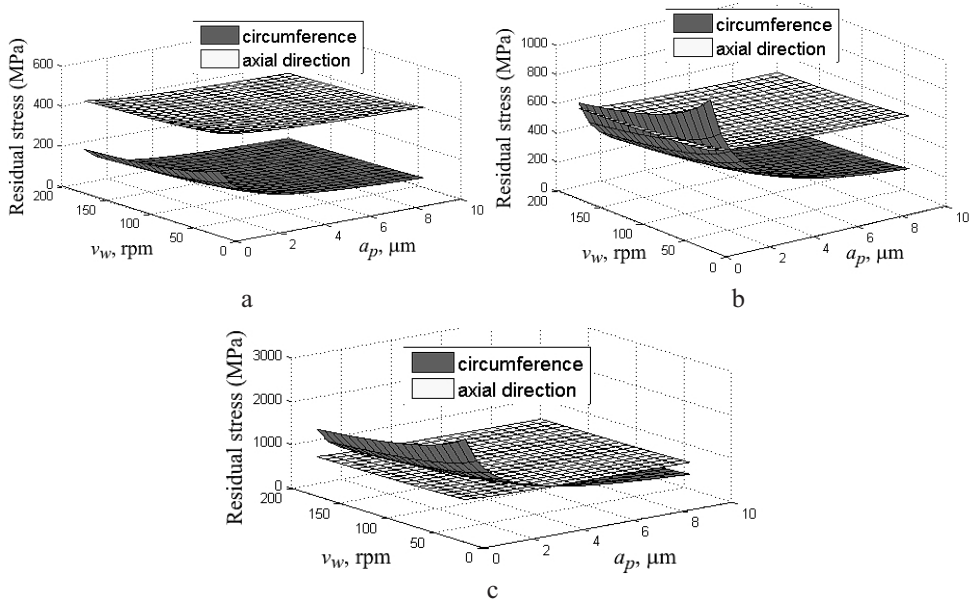Fig. 4. The residual stress at the different cutting depth a_p: (a) $a_p = 1\,\mu$m; (b) $a_p = 3\,\mu$m; (c) $a_p = 5\,\mu$m.

Fig. 5. The residual stress at the different grinding wheel speed v_s: (a) $v_s = 45$ m/s; (b) $v_s = 94$ m/s; (c) $v_s = 150$ m/s.

the information forward transfer and the error back propagation, thus it can ensure the output layer achieve the desired goal [13].

4.1. Design of BP Network. The BP algorithm has some shortcomings, including that the network has a slow convergence speed in the learning process and it is easy to converge to the local minimum. So the network training with adaptive learning rate [14] is adopted to increase BP algorithm for forecasting the surface residual stress in grinding titanium alloy.

The learning rate value of BP neural network ranges from 0 to 1. The bigger it is, the more obvious the change of the weight and the faster the learning rate of the network are. When the learning rate is too high, the oscillation will be produced in the weight training process. However, when it is too low, the convergence speed of the network will be very slow, which can make quite problematic the task of attaining a stable value by the weight . For this problem, selecting the appropriate learning rate is not easy. The latter rate is usually obtained via experiments, and although the learning rate may provide a good efficacy in the early training, it is not necessarily suitable for the subsequent training. In order to solve this problem, the adjustment of adaptive learning rate based on Eq. (8) in the training process is quite important

$$\eta(k+1) = \begin{cases} 1.05\eta(k), & SSE(k+1) < SSE(k), \\ 0.7\eta(k), & SSE(k+1) > 1.04 SSE(k), \\ \eta(k), & \text{else}, \end{cases} \tag{8}$$

where $\eta(k)$ is the learning rate for the kth time and $SSE(k)$ is the square sum of error for the kth time.

Since the relationship between the surface residual stress and the grinding conditions is fairly complicated, the BP network with double hidden layers is constructed to achieve precise forecasting results. The input values of network are the grinding wheel speed v_s, workpiece speed v_w, and cutting depth a_p, so the input layer of the network has three neurons. Based on the Kolmogorov theorem [15], the middle layer of network can include seven neurons. The output value of the network is the surface residual stress. Figure 6 shows the BP neural network model, which meets the above requirements. Neurons transfer functions of network hidden layer are "tansig" S-tangent function, and the output layer neuron uses a "purelin" linear transfer function.

The importation of network is a three-dimensional vector with different dimensions, therefore the experimental data must be normalized firstly to eliminate the dimensions of different conditions for the fast convergence speed of the prediction network and ensure that the network converges quickly.
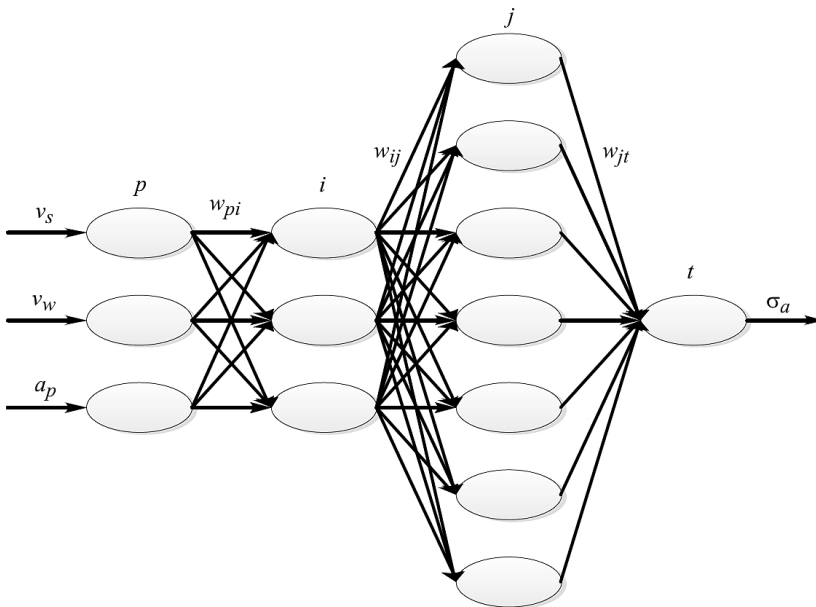

Fig. 6. BP network with double hidden layers.

The joint normalization method [16] is used to increase the correlation between different characteristic parameters. The same grinding parameters in different experiment groups (column vector) are normalized first and a normalization matrix of the column vector is created. Then, the row vector of the normalized matrix is used to normalize and a normalization matrix of row vector is made. Joint normalization method processes the data according to the Eq. (9)

$$x' = 2\frac{x - x_{\min}}{x_{\max} - x_{\min}} - 1, \tag{9}$$

where x is the input vector, $x_{\min}$ is the minimum element of x, $x_{\max}$ is the maximum element of x, and x' is the normalization result of x.

4.2 Network Training and Analysis of the Prediction Result of the Residual Stress. In order to improve the forecasting accuracy of the residual stress, this experiment sets the maximum training number as 50,000 and the target accuracy of training as 0.0001. The trained network is used to predict the results of the above 5 groups of grinding experiments.

Obtained by the different training methods with various normalization methods, the simulation results are shown in Table 2, which indicates that the network trained by the adaptive learning rate is significantly better than that trained by the fixed learning rate, while the joint normalized network is more efficient and stable network with faster convergence and fewer iterations.

T a b l e 2

Circumferential and Axial Simulation Results of BP Network for the Above 5 Groups Experimental Data

Training methods		Normalization methods			
		Circumferential		Axial	
		Conventional	Jointed	Conventional	Jointed
Fixed learning rate	Average error (%)	6.8956	8.0642	47.747	45.590
	Iterations	9573	6001	10199	6329
Adaptive learning rate	Average error (%)	2.3400	1.4770	6.217	2.756
	Iterations	5670	2909	6404	2239

Figure 7 illustrates the comparative analysis of the errors of surface residual stresses calculated by the empirical model, the conventional normalized network, and the joint normalized one.

In general, the axial values predicted by the above three methods are more accurate than the circumferential ones. The error of the empirical model is the maximal among these methods. Moreover, the range of the circumferential error is between 1.335 and 26.997% while the axial error is between 0.18 and 6.112%.

The relationship between the surface residual stresses and grinding conditions is so complex that it cannot be described by a single exponential relationship. Therefore, the empirical model is not precise enough in some situations. BP network has a good capability of nonlinear mapping and self-learning, which can describe the complex relationship accurately. The prediction error of circumferential residual stress reaches 23.496% in the first set of grinding parameters, while all other errors are less than 5.2%.

Due to the use of joint normalization algorithm, its predictive value is the most accurate, whereas the axial error is in the range from 0.388 to 2.532% and the circumferential
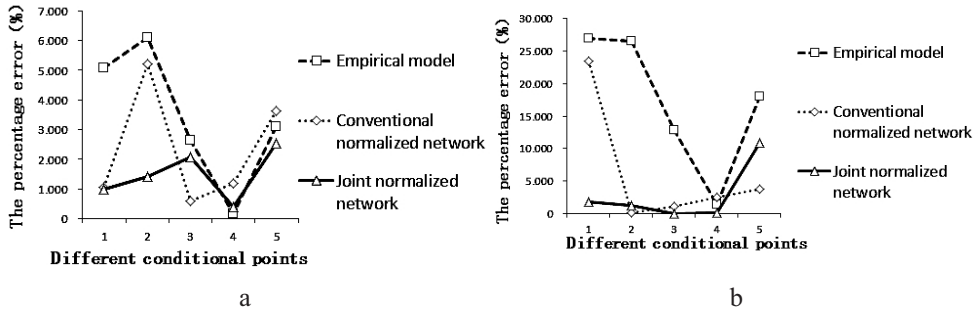
Fig. 7. The comparative analysis results by three different methods: (a) axial; (b) circumferential.

error is in the range from 0.009 to 10.811%. The accuracy is increased by 56.851 and 83.941%, as compared to the predictive values of the empirical model.

Conclusions. This paper presents a study on the relationship between surface residual stresses and grinding conditions in the process of high-speed cylindrical grinding of titanium alloy with super abrasive CBN grinding wheels. The experimental results obtained show that the grinding wheel speed v_s has a strong influence on the residual stresses of titanium alloys: especially when the wheel speed reaches 60 m/s, the compressive residual stress increases sharply. This implies that high-speed grinding technology has broad application prospects in machining of titanium alloys.

The empirical model is determined by identifying its parameters. The feasibility and accuracy of empirical model are verified, and the basis for the grinding conditions selection is provided for a certain grinding process of titanium alloys. Meanwhile, the effectiveness of adaptive learning rate BP network is also indicated, which corroborates its applicability in engineering practice.

It can be shown that the increases of circumferential residual stress benefits from high grinding wheel speed v_s and large cutting depth a_p. A low grinding wheel speed v_s and large cutting depth a_p contribute to the increase in the axial residual stresses. This experimental results can provide a reliable reference for the selection of grinding conditions.

1. D. Y. Jang, T. R. Watkins, K. J. Kozaczek, et al., "Surface residual stresses in machined austenitic stainless steel," *Wear*, **194**, No. 1-2, 168–173 (1996).

2. D. J. Shen, J. R. Cai, C. H. Guo, and P. Y. Liu, "Evolution of residual stresses in micro-arc oxidation ceramic coatings on 6061 Al alloy," *Chin. J. Mech. Eng.*, **6**, 1149–1153 (2013).

3. Z. C. Lin and B. Y. Lee, "An investigation of the residual stress of a machined workpiece considering tool flank wear," *J. Mater. Process. Technol.*, **51**, No. 1-4, 1–24 (1995).

4. K. C. Ee, O. W. Dillon, and I. S. Jawahir, "Finite element molding of residual stresses in machining induced by cutting using a tool with finite edge radius," *Int. J. Mech. Sci.*, **47**, Issue 10, 1611–1628 (2005).

5. M. Vosough, V. Kalhori, P. Liu, and I. Svenningsson, "Influence of high pressure water-jet assisted machining on surface residual stresses on Ti–6Al–4V alloy by measurement and finite element simulation," in: Proc. of the 3rd Int. Surface Engineering Conf. (2004), pp. 107–113.

6. R. K. Kang and J. X. Ren, "An effective way to improve the grinding residual stress of titanium," *Aeronaut. Manufact. Technol.*, No. 2, 7–11 (1990).

7. Z. H. Hu and Z. J. Yuan, "Research on the forming mechanism of residual stresses produced in grinding of residual stresses produced in grinding," *J. Harbin Inst. Technol.*, No. 3, 51–60 (1989).

8. J. X. Ren and X. B. Wang, *Grinding Technology of Difficult-to-Machine Materials*, Publishing House of Electronics Industry (2011).

9. G. Yoneya, in: J. Zhu and H. M. Shao (Eds.), *The Produce and Countermeasure of Residual Stress*, China Machine Press, Beijing (1983), pp. 210–214

10. C. Z. Zhang, D. M. Li, S. P. Pang, and S. J. Guan, "Study on the interior residual stress of metal surveyed by x-ray method," *J. Jilin Inst. Chem. Technol.*, **18**, No. 4, Dec (2001).

11. E. Brinksmeier, J. T. Cammett, W. König, et al., "Residual stresses – measurement and causes in machining processes," *CIRP Annals – Manufact. Technol.*, **31**, Issue 2, 491–510 (1982).

12. X. C. Wang, F. Shi, L. Yu, and Y. Li, *MATLAB Neural Network Analysis of 43 Cases* [Chinese edition], Beijing University of Aeronautics and Astronautics Press, Beijing (2013).

13. F. Shi, S. C. Wang, L. Yu, and Y. Li, *MATLAB Neural Network Analysis of 30 Cases* [Chinese edition], Beijing University of Aeronautics and Astronautics Press, Beijing (2010).

14. D. F. Zhang, *Application in the Design of Neural Networks Using MATLAB*, China Machine Press, Beijing, (2009).

15. N. V. Krylov, *Introduction to the Theory of Random Processes*, American Mathematical Society (2002).

16. X. T. Liu, "Study on data normalization in BP Neural Network," *Mech. Eng. Automat.*, **3**, 122–126 (2010).